

Gaussian Grouping: Segment and Edit Anything in 3D Scenes

Mingqiao Ye Martin Danelljan Fisher Yu Lei Ke ♠
 ETH Zürich
 ♠ Project Lead

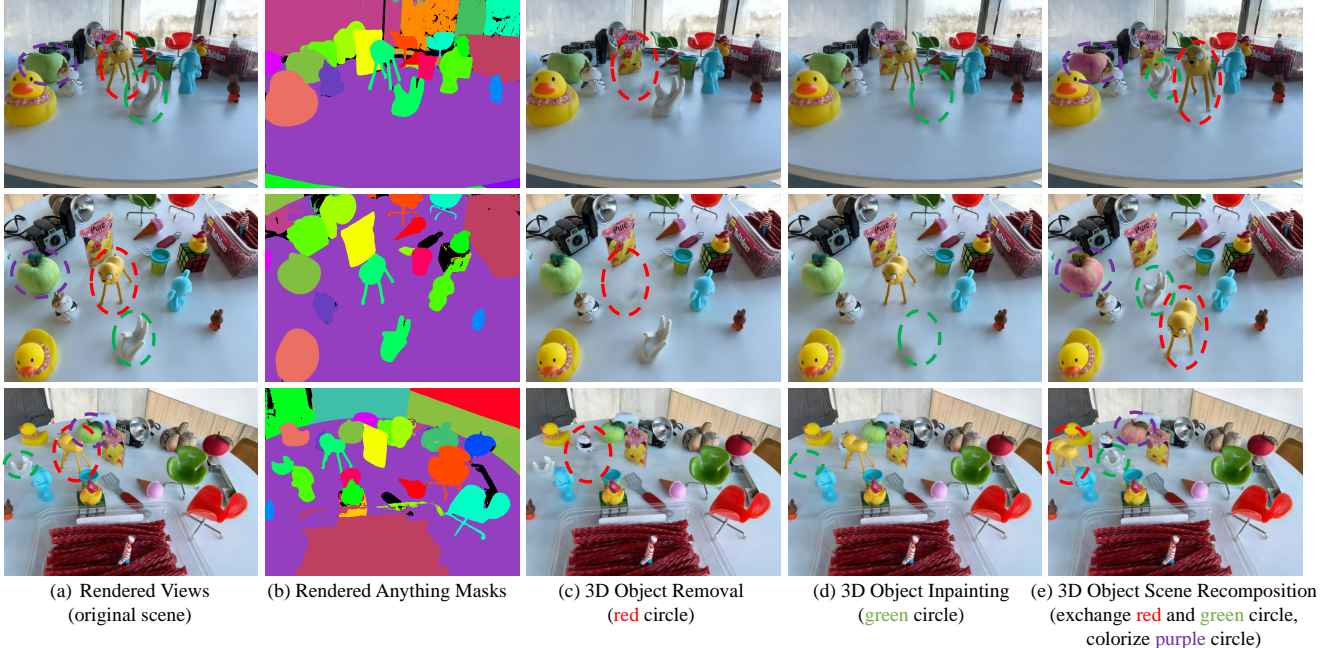


Figure 1. Our Gaussian Grouping approach jointly reconstructs (column a) and segments (column b) anything in full open-world 3D scenes, with fine-grained instance and stuff level modeling. This enables versatile scene editing applications, such as 3D object removal (column c), 3D object inpainting (column d) and scene re-composition and object colorization (column e). Since the segmentation information is encapsulated in the 3D Gaussians, editing tasks such as 3D object removal, colorization and object location exchange can be performed directly w/o training, while inpainting only requires minutes of fine-tuning.

Abstract

The recent Gaussian Splatting achieves high-quality and real-time novel-view synthesis of the 3D scenes. However, it is solely concentrated on the appearance and geometry modeling, while lacking in fine-grained object-level scene understanding. To address this issue, we propose Gaussian Grouping, which extends Gaussian Splatting to jointly reconstruct and segment anything in open-world 3D scenes. We augment each Gaussian with a compact Identity Encoding, allowing the Gaussians to be grouped according to their object instance or stuff membership in the 3D scene. Instead of resorting to expensive 3D labels, we supervise the Identity Encodings during the differentiable rendering by leveraging the 2D mask predictions by SAM, along with introduced 3D spatial consistency regularization. Comparing to the implicit NeRF representation, we show that the dis-

crete and grouped 3D Gaussians can reconstruct, segment and edit anything in 3D with high visual quality, fine granularity and efficiency. Based on Gaussian Grouping, we further propose a local Gaussian Editing scheme, which shows efficacy in versatile scene editing applications, including 3D object removal, inpainting, colorization and scene re-composition. Our code and models will be at <https://github.com/1keab/gaussian-grouping>.

1. Introduction

Open-world 3D scene understanding is an essential challenge, with far-reaching implications for robotics, AR / VR, and autonomous driving. Given a set of posed RGB images, our goal is to learn an effective 3D representation that jointly reconstructs and segments anything in the 3D scene. The representation should easily support a wide range of

downstream scene editing applications. For example, in Figure 1, the 3D object of the scene can be easily removed or inpainted, and the scene can be recomposed by exchanging multiple object locations.

While there has been remarkable progress in 2D scene understanding brought by SAM and its variants [12, 15, 58], their extension to 3D has been constrained. This is mostly by the availability and the labor-intensive process of creating 3D scene datasets. Existing methods [8, 37] rely on manually-labeled datasets, which are both costly and limited in scope, or requires accurately scanned 3D point clouds [33, 42] as input. This hinders the development of the 3D scene understanding approaches that can quickly generalize across various real-world scenes.

By taking multi-view captures, existing NeRFs-based methods [14, 17, 25, 39] lift 2D masks or distill CLIP [34] / DINO [3] features via neural fields rendering. However, due to the implicit and continuous representation of NeRF, these methods require expensive random sampling and are computationally intensive to optimize. Further, it is hard to directly adjust NeRF-based approaches for the downstream local editing tasks [17], because the learned neural networks, such as MLPs, cannot decompose each part or module in the 3D scene easily. Several methods [4, 38] combine NeRF or stable-diffusion [36] with the masks of SAM, but they focus on a single object without attaining more holistic scene understanding.

Alternative to NeRFs, the recently emerged 3D Gaussian Splatting [13] has shown impressive reconstruction quality with high training and rendering efficiency. It represents the 3D scene with an array of coloured and explicit 3D Gaussians, which are rendered into camera views for novel view synthesis. Nevertheless, Gaussian Splatting does not model object instance or semantic understanding. To achieve fine-grained scene understanding, we extend this approach beyond merely capturing the scene’s appearance and geometry to include the individual objects and elements that constitute the 3D environments.

We propose *Gaussian Grouping*, which represents the whole 3D scene with a set of grouped 3D Gaussians. By inputting multi-view captures and the corresponding automatically generated masks by SAM, our method learns a discrete and grouped 3D representation for reconstructing and segmenting anything in the 3D scene. Gaussian Grouping inherits SAM’s strong zero-shot 2D scene understanding capability and extends it to the 3D space by producing consistent novel view synthesis and segmentation.

To this end, instead of solely modeling the scene appearance and geometry, our approach also captures the identity of each Gaussian of the 3D scene by grouping. A new property, our *Identity Encoding*, is augmented to each Gaussian. The Identity Encoding is a compact and low-dimensional learnable embedding. To leverage the segmentation super-

vision in 2D, Identity Encoding is trained via differentiable Gaussian rendering, where the encoding vectors of various Gaussians are splatted onto the 2D rendering view. Then, we take the 2D rendered identity features and employ an extra linear layer to classify these splatted embeddings on each 2D location for identity classification.

To further boost the grouping accuracy, besides the standard cross-entropy loss for identity classification, we also introduce an **un**-supervised 3D Regularization Loss by leveraging 3D spatial consistency. The loss enforces the Identity Encodings of the top K -nearest 3D Gaussians to be close in their feature distance. We find it helps for Gaussians inside the 3D object or heavily occluded to be supervised during rendering more sufficiently.

We highlight the advantages of Gaussian Grouping not only by providing high visual quality and fast training, but also through its downstream scene editing applications brought by our dense 3D segmentation. Since our model captures the 3D scenes as compositional structures, each Gaussian group within the scene operates independently, allowing for parts to be fully decoupled or separated. This decomposition is crucial in scenarios where individual components need to be identified, manipulated, or replaced without disrupting the entire scene structure. We also propose an efficient Local Gaussian Editing strategy based on the grouping. By the grouped 3D Gaussians, we show extensive 3D scene editing cases, such as in 3D scene re-composition, object inpainting or object removal, with both impressive visual effect and fine granularity.

2. Related Works

3D Gaussian Models 3D Gaussian Splatting [13] has recently emerged as a powerful approach to reconstruct 3D scenes via real-time radiance field rendering. Several follow-up methods [26, 52, 53] extend it to dynamic 3D scenes by tracking of all dense scene elements [26] or deformation field modeling [49, 52]. Another stream of works [6, 43, 54] focus on the 3D content creation, which combine Gaussian Splatting with the diffusion-based models and show high-quality generation results. However, none of the existing Gaussian Splatting works enables object / stuff-level or semantic understanding of the 3D scene. Our Gaussian Grouping extends Gaussian Splatting from pure scene appearance and geometry modeling to also support open-world and fine-grained scene understanding. We show that the grouped 3D Gaussians is an effective and flexible 3D representation in supporting a series of downstream scene editing applications.

Radiance-based Open World Scene Understanding Existing semantic scene modeling approaches combined with radiance fields are NeRF-based [29]. Semantic-NeRF [60] initiated the incorporation of semantic information into NeRFs and facilitated the generation of semantic masks

from novel views. Building upon it, subsequent research focusing on in-domain scene modeling, has expanded the scope by introducing instance modeling [9, 20, 39, 47] or encoding visual features [17, 35, 44–46] that support semantic delineation. Unlike our approach, most of these methods are designed for in-domain scene modeling and cannot generalize to open-world scenario.

By distilling 2D features such as CLIP [34] or DINO [3], Distilled Feature Fields [17] explores embedding pixel-aligned feature vectors, and LERF [14] learns language field to help open-world 3D semantics. In contrast to our work, these open-world approaches are only limited in semantic segmentation (hard to separate similar objects of the same category) and cannot produce very accurate segmentation masks as shown in our experiment. To our knowledge, we propose the first Gaussian-based method to tackle open-world 3D scene understanding, where we show the advantages comparing to existing NeRF-based approaches [14, 17, 39] in segmentation quality, efficiency and good extension to downstream scene editing applications.

SAM in 3D Segment Anything Model (SAM) [15] was released as a foundational vision model for zero-shot 2D segmentation. Several works lift SAM’s 2D masks to 3D segmentation via NeRF [4, 5] or 3D point cloud [51]. However, these NeRF-based approaches only focus on single / few objects of the 3D scene, while our Gaussian Grouping operates in automatic *everything* mode to attain the holistic understanding of each instance / stuff of the full scene.

Radiance-based Scene Editing Manipulating 3D scenes via radiance field is challenging. For existing NeRF-based scene editing / manipulation works [11, 22, 23, 57], Clip-NeRF [48], Object-NeRF [50], and LaTeRF [30] design approaches to change and complete objects represented by NeRFs; however, their application scenario is limited to simple objects, rather than scenes with significant clutter and texture. Some other works specify bounding boxes [32, 56], to allow flexible compositing of various objects [59] or combining with physical simulation [21]. Mostly recently, 3D object inpainting is studied in SPIn-NeRF [31] and language-based scene editing is proposed in [10]. Compared to them, we apply our Gaussian Grouping to versatile scene editing tasks, and show benefits brought by the fine-grained scene modeling, where multiple scene editings can be easily superimposed on the same image. The design of Local Gaussian Editing makes the whole training / editing process both simple and efficient.

3. Method

Our work aims to build an expressive 3D scene representation, which not only models appearance and geometry, but also captures every instance and stuff identity of the scene. We design our method based on the recent 3D Gaussian Splatting [13], and extend it from pure 3D reconstruction

to fine-grained scene understanding. Our approach, called *Gaussian Grouping*, is capable of: 1) modeling each 3D part of the scene with appearance, geometry together with their mask identities; 2) fully decomposing the 3D scene into discrete *groups*, *e.g.* representing different object instances; 3) allowing for fast training and rendering, while not diluting the original 3D reconstruction quality.

Gaussian Grouping effectively leverages the dense 2D mask proposals of SAM, and lifts them to segment anything in the 3D scene via radiance fields rendering. In Sec 3.1, we first briefly review the 3D Gaussian Splatting method on radiance field rendering. We then detailed the input data pre-processing steps in Section 3.2.1, and further described the propose Gaussian Grouping in Section 3.2.2. With the constructed 3D representation, finally, we show its advantages in downstream scene editing tasks by the efficient Local Gaussian Editing in Section 3.3.

3.1. Preliminaries: 3D Gaussian Splatting

Gaussian Splatting, as introduced by Kerbl et al. [13], encapsulates 3D scene information using a suite of 3D colored Gaussians. This technique has established its effectiveness in the reconstruction tasks, exhibiting high inference speeds and remarkable quality of reconstruction within timeframes on par with those of NeRF. Yet, its potential in scene understanding has not been thoroughly investigated. Our research reveals that 3D Gaussians hold considerable promise for the open-world and complex 3D scene understanding.

To represent the scene, each Gaussian’s property is characterized by a centroid $\mathbf{p} = \{x, y, z\} \in \mathbb{R}^3$, a 3D size $\mathbf{s} \in \mathbb{R}^3$ in standard deviations, and a rotational quaternion $\mathbf{q} \in \mathbb{R}^4$. To allow fast α -blending for rendering, we assign an opacity value $\alpha \in \mathbb{R}$ and a color vector \mathbf{c} represented in the three degrees of spherical harmonics (SH) coefficients. These adjustable parameters are collectively symbolized by S_{Θ_i} , where $S_{\Theta_i} = \{\mathbf{p}_i, \mathbf{s}_i, \mathbf{q}_i, \alpha_i, \mathbf{c}_i\}$ represents the set of parameters for the i -th Gaussian. To visualize and supervise these 3D Gaussians, Gaussian Splatting projects them onto the 2D image plane. It implements differentiable rendering and gradient-based optimization for each pixel in a sequence of Gaussians sorted in the depth order, for computing the final color and opacity.

3.2. 3D Gaussian Grouping

In this section, we describe the design of our Gaussian Grouping. To enable 3D Gaussians for fine-grained scene understanding, our key insight is that we preserve all attributes of the Gaussians (such as their number, color, opacity, and size) in its original setting, but add new Identity Encoding parameters (similar to the format of color modeling). This allows each Gaussian to be assigned to its represented instances or stuffs in the 3D scene.

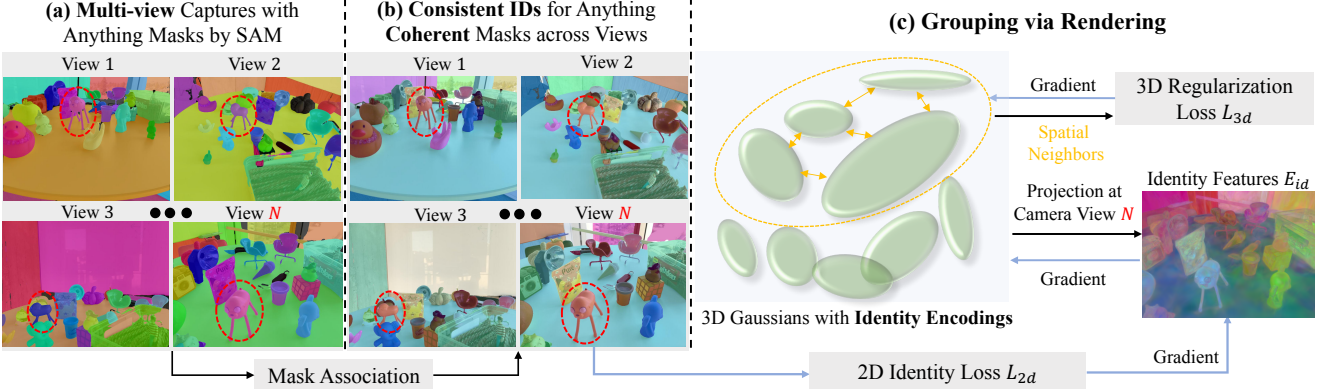


Figure 2. The method pipeline of our Gaussian Grouping contains three main steps: (a) We first prepare the input by deploying SAM to automatically generate masks in *everything* mode for each view independently. (b) Then, to obtain the consistent masks IDs across training views, we take an universal temporal propagation model [7] to associate the mask labels and generate a coherent multi-view segmentation. (c) With the prepared training input, we jointly learn all properties of the 3D Gaussians, including their group Identity Encoding, by differentiable rendering. Our encoding is supervised by the 2D Identity Loss, leveraging the coherent segmentation views, and a 3D Regularization loss. We use color to denote object IDs across frames for input views. We omit the rendering process for other Gaussian parameters and the density control part for simplicity, as it is inherited from [13].

3.2.1 Anything Mask Input and Consistency

To model open-world scenes, instead of relying on the expensive 3D labels for supervision, we train our approach by utilizing SAM’s 2D masks [15] as input. Concretely, we take a set of multi-view captures along with the automatically generated 2D segmentations by SAM, as well as the corresponding cameras calibrated via SfM [40]. SAM is adopted here because it shows strong zero-shot capabilities not limited by the training categories, and supports automatically segmenting *everything* in a wide-variety of images.

2D Image and Mask Input To prepare the input for Gaussian Grouping, in Figure 2 (a), we first deploy SAM to automatically generate masks for each image of the multi-view collection. The 2D masks are individually produced per image. Then, to assign each 2D mask a unique ID in the 3D scene, we need to associate the masks of the same identity across different views and obtain the total number K of instances / stuffs the 3D scene.

Identity Consistency across Views Instead of resorting to the cost-based linear assignment [39] during training, we treat the multi-view images of a 3D scene as a video sequence with gradually changing views. To achieve the 2D mask consistency across views, we employ a well-trained zero-shot tracker [7] to propagate and associate masks. This also provides the total number of mask identities in the 3D scene. We visualize associated 2D mask labels in Figure 2 (b). Comparing to the cost-based linear assignment proposed in [39], we find it simplifies the training difficulty while avoids repeatedly compute the matching relation in each rendering iteration, resulting over $60\times$ speeding up. It also achieves better performance than the cost-based linear assignment, especially under the dense and overlapping masks by SAM.

3.2.2 3D Gaussian Rendering and Grouping

Conventional 3D Gaussian parameters for modeling the scene includes 3D center position (mean), 3D size (anisotropic covariance), opacity, and color (Spherical Harmonic coefficients). Separate operations are taken for the adaptive control on the Gaussian density. As in Sec 3.1, these properties are differentiable and can be easily projected to 2D splats for the whole scene optimization.

Identity Encoding To generate 3D-consistent mask identities across views of the scene, we propose to group 3D Gaussians belong to the same instance / stuff. In addition to the existing Gaussian properties, we introduce a new parameter, i.e., Identity Encoding, to each Gaussian. The Identity Encoding is a learnable and compact vector of length 16, which we find is sufficient to distinguish the different objects / parts in the scene with computation efficiency. During training, similar to Spherical Harmonic (SH) coefficients on representing color of each Gaussian, we optimize the introduced Identity Encoding vector to represent its instance ID of the scene in the same manner. However, different from the view-dependent appearance modeling of the scene, the instance ID is consistent across various rendering views. Thus, we set the SH degree of the Identity Encoding to 0, only to model its direct-current component. Unlike NeRF-based methods [14, 17, 39] designing extra semantic MLP layers, the Identity Encoding serves as the learnable property for each Gaussian to group the 3D scene.

Grouping via Rendering To optimize the introduced Identity Encoding of each Gaussian, in Figure 2 (c), we render these encoded identity vectors into 2D images in a differentiable manner. We take the differentiable 3D Gaussian renderer from [13] and treat the rendering process similar to the color (SH coefficients) optimization in [13].

3D Gaussian splatting adopts neural point-based α' -rendering [18, 19], where the influence weight α' can be evaluated in 2D for each pixel for each Gaussian. Following [13], the influence of all Gaussians on a single pixel location are computed by sorting the Gaussians in depth order and blending \mathcal{N} ordered points overlapping the pixels [27, 29]:

$$E_{\text{id}} = \sum_{i \in \mathcal{N}} e_i \alpha'_i \prod_{j=1}^{i-1} (1 - \alpha'_j) \quad (1)$$

where the final rendered 2D mask identity feature E_{id} for each pixel is a weighted sum over the Identity Encoding e_i of length 16 for each Gaussian, weighted by the Gaussian's influence factor α'_i on that pixel. Refer to [55], we compute α'_i by measuring a 2D Gaussian with covariance Σ^{2D} multiplied with a learned per-point opacity α_i , and

$$\Sigma^{2D} = JW\Sigma^{3D}W^T J^T \quad (2)$$

where Σ^{3D} is the 3D covariance matrix, Σ^{2D} is the splatted 2D version [61]. J is the Jacobian of the affine approximation of the 3D-2D projection, and W is the world-to-camera transformation matrix.

Grouping Loss After associating 2D instance labels across each training view (Sec 3.2.1), suppose there are K masks in total in the 3D scene. To group each 3D Gaussian by the instance /stuff mask identities, we design the grouping loss \mathcal{L}_{id} for updating the Identity Encoding of Gaussians with two components:

1) **2D Identity Loss**: Since the mask identity labels are in 2D, instead of directly supervising the Identity Encoding e_i of the 3D Gaussians. Given the rendered 2D features E_{id} in Eq. 1 as input, we first add a linear layer f to recover its feature dimension back to $K+1$ and then take $\text{softmax}(f(E_{\text{id}}))$ for identity classification, where K is the total number of masks in the 3D scene. We adopt a standard cross-entropy loss \mathcal{L}_{2d} for $K+1$ categories classification.

2) **3D Regularization Loss**: To further boost the grouping accuracy of Gaussians, besides the standard cross-entropy loss for indirect 2D supervision, we also introduce an unsupervised 3D Regularization Loss to directly regularize the learning of Identity Encoding e_i . 3D Regularization Loss leverages the 3D spatial consistency, which enforces the Identity Encodings of the top k -nearest 3D Gaussians to be close in their feature distance. This allows the 3D Gaussians inside the 3D object, or heavily occluded (not visible in nearly all training views) during the point-based rendering (Eq. 1) being supervised more sufficiently. In Eq. 3, we denote F as softmax operation combined after linear layer f (shared in computing the 2D Identity loss). We formalize the KL divergence loss with m sampling points as,

$$\mathcal{L}_{3d} = \frac{1}{m} \sum_{j=1}^m D_{\text{kl}}(P || Q) = \frac{1}{mk} \sum_{j=1}^m \sum_{i=1}^k F(e_j) \log \left(\frac{F(e_j)}{F(e'_i)} \right) \quad (3)$$

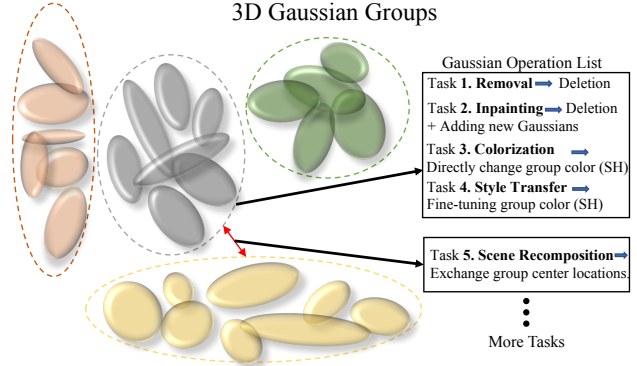


Figure 3. The grouped 3D Gaussians after training, where each group represents a specific instance / stuff of the 3D scene and can be fully decoupled. Our representation is efficient to support versatile downstream scene editing applications, where we design a Gaussian Operation List consists of simple operations like group deletion, group addition, finetuning Spherical Harmonic (SH) and exchanging 3D center locations.

where P contains the sampled Identity Encoding e of a 3D Gaussian, while the set $Q = \{e'_1, e'_2, \dots, e'_k\}$ consists of its k nearest neighbors in 3D spatial space. We omit the softmax operation combined after linear layer f for simplicity.

Training Objective Combined with the conventional 3D Gaussian Loss \mathcal{L}_{ori} on image rendering [13], the total loss $\mathcal{L}_{\text{render}}$ for fully end-to-end training is

$$\mathcal{L}_{\text{render}} = \mathcal{L}_{\text{ori}} + \mathcal{L}_{\text{id}} = \mathcal{L}_{\text{ori}} + \lambda_{2d}\mathcal{L}_{2d} + \lambda_{3d}\mathcal{L}_{3d} \quad (4)$$

3.3. Local Gaussian Editing

After the 3D Gaussian field training and grouping (Sec 3.2.2), as in Figure 3, we represent the whole 3D scene with a set of grouped 3D Gaussians. To perform various downstream local scene editing tasks, we propose the efficient Local Gaussian Editing. Thanks to the decoupled scene representation, instead of finetuning all 3D Gaussians, we freeze the properties for the most of the well-trained Gaussians and only adjust a small part of existing or newly added 3D Gaussians relevant to the editing targets. For 3D object removal, we simply delete the 3D Gaussians of the editing target. For 3D scene re-composition, we exchange the 3D location between two Gaussian groups. These two editing applications are direct with no parameter tuning.

For 3D object inpainting, we first delete the relevant 3D Gaussians and then add a small number of new Gaussians to be supervised by the 2D inpainting results by LAMA [41] during rendering. For 3D object colorization or style transfer, we only tune the color (SH) parameters of the corresponding Gaussian group, while fixing the 3D positions and sizes of them to preserve the learned 3D scene geometry.

The proposed local Gaussian editing scheme is time efficient, as shown in our experiment. Because of our fine-grained masks modeling, it also supports multiple con-

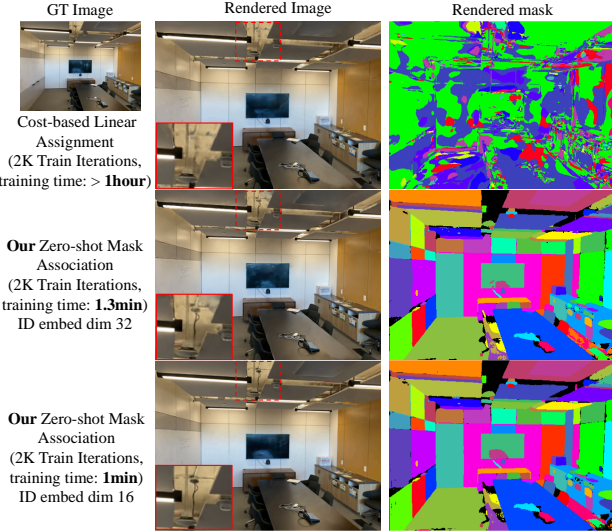


Figure 4. Ablation on the Identity Consistency across views, where we treat multi-view images as a video and associate the mask labels to generate a coherent segmentation labels [7] for training. We compare our rendering results (the 3rd row) to using cost-based linear assignment [39] during training (the 1st row), but found it leads to slow training and inferior testing performance in both reconstruction and segmentation.

current local editings without interfering with each other or re-training the whole global 3D scene representation with new editing operation. Comparing to NeRF-based approaches [10, 17, 31], we show extensive visual comparisons for versatile scene editing cases in our experiment section and the Supp. file.

4. Experiments

4.1. Dataset and Experiment Setup

Datasets To measure to segmentation or fine-grained localization accuracy in open-wold scene, we evolve the existing LERF-Localization [14] evaluation dataset and propose the LERF-Mask dataset, where we manually annotate three scenes from LERF-Localization with accurate masks instead of using coarse bounding boxes. For each 3D scene, we provide 7.7 text queries with corresponding GT mask label in average, more details are provided in the Supp. file.

To evaluate the reconstruction quality, we tested our Gaussian Grouping on 7 of full 9 sets of scenes presented in Mip-Nerf360 [1], where the flowers and treehill are skipped due to the non-public access right. We also take diverse 3D scene cases from LLFF [28], Tanks&Temples [16] and Instruct-NeRF2NeRF [10] for visual comparison. We also adopt boundary metrics mIoU for better segmentation quality measurement.

Implementation Details We implement Gaussian Grouping based on Gaussian Splatting [13]. We add an 16 dimension identity encoding as a feature of each Gaussian and

Table 1. Comparison of Open Vocabulary Segmentation on LERF-Mask dataset. To compare fine-grained mask localization quality, we annotate the test views of three 3D scenes from LERF-Localization [14] dataset with accurate masks to replace its original coarse bounding boxes. We adopt the detected box from Grounding DINO [24] to select the mask ID in a 3D scene.

Model	figurines		ramen		teatime	
	mIoU	mBIOU	mIoU	mBIOU	mIoU	mBIOU
LERF [14]	33.5	30.6	28.3	14.7	49.7	42.6
Gaussian Grouping	69.7	67.9	77.0	68.7	71.7	66.1

Table 2. Ablation of Identity Encoding on Mip-NeRF 360 [1] dataset with its seven public scenes. The joint training of the introduced Identity Encodings with original Gaussian parameters does not hurt the original Gaussians reconstruction quality.

Model	Identity	PSNR \uparrow	SSIM \uparrow	LPIPS \downarrow	FPS
Gaussian Splatting [13]		28.69	0.870	0.182	\sim 200
Gaussian Grouping	✓	28.43	0.863	0.189	\sim 170

implement forward and backward cuda rasterization similar to rgb feature. The output classification linear layer has 16 input channels and 256 output channels. In training, $\lambda_{2d} = 1.0$ and $\lambda_{2d} = 2.0$. We use the Adam optimizer for both gaussians and linear layer, with a learning rate of 0.0025 for identity encoding and 0.0005 for linear layer. For 3D regularization loss, we choose $k = 5$ and $m = 1000$. All datasets are trained for 30K iterations on one A100 GPU.

For 3D object removal, we obtain the 3D Gaussians with classification of the selected instance id. Post-processing involves first removing the outliers and then using a convex hull to get all Gaussians corresponding to the object for deletion. For 3D object inpainting, we initialize Gaussians near the deletion region and finetune with the same LPIPS loss in inpainting mask as SPIn-NeRF [31].

4.2. Multiview Reconstruction and Segmentation

Ablation on Mask Cross-view Association To study the effect of cross-view masks association [7] for input preparation, we replace the associated masks input to the individual masks predicted by SAM per image in Gaussian Grouping. We take the cost-based linear assignment strategy proposed in [39], and perform the visual comparison on rendering results in Figure 4. The linear assignment not only heavily slows down the whole training due to the assignment computation in each iteration, but also produces noised mask predictions. This is owing to the large gradients brought by the unstable cost-based liner assignment, especially at the initial training stage of the network, where masks prediction is nearly random. For 2K training iteration, linear assignment requires 1 hour but our associated mask input only requires 1 minute. Also, we compare the scene render reconstruction quality in Figure 4, where the appearance details of the rope attached to the ceiling (see the zoom region) is much better preserved by our method.

Open-vocabulary Segmentation Comparison We compare the segmentation quality of Gaussian Grouping in

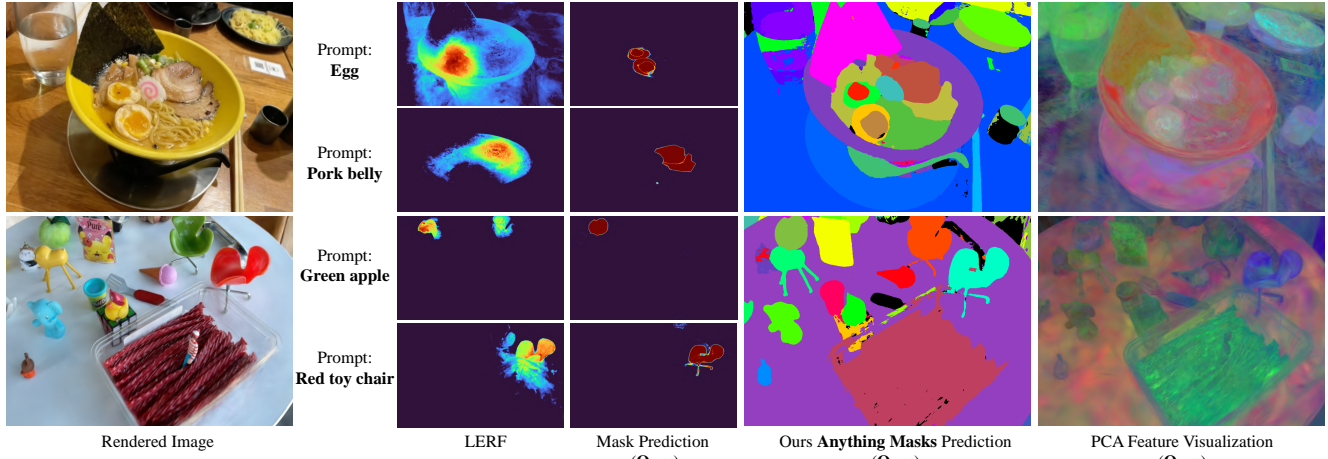


Figure 5. Segmentation comparison between LERF [14] and our Gaussian Grouping on the rendering view. The masks predicted by Gaussian Group contains much sharp and accurate boundary than LERF. Also, our approach is better at distinguish objects with similar colors, such as the “Green apple” prompt case. We input the corresponding text queries to Grounding DINO [24] to select the mask ID from our Anything Masks prediction. We adopt PCA to visualize the rendered Identity Encoding features in the rightmost column.

3D scenes with existing open-vocabulary 3D segmentation method, such as LERF [14]. In Table 1, the advantage of our Gaussian Grouping is significant, doubling the performance of LERF on both the “figurines” and “ramen” scenes. We also show the visual segmentation comparison in Figure 5, where the segmentation prediction by our method is much more accurate with clear boundary, while LERF-based similarity computing methods only provide a rough localization area. Since SAM does not support language prompt, we adopt the Grounding DINO [24] to identify the mask ID in a 2D image, and then pick the corresponding mask from our anything masks prediction (2nd column from the right).

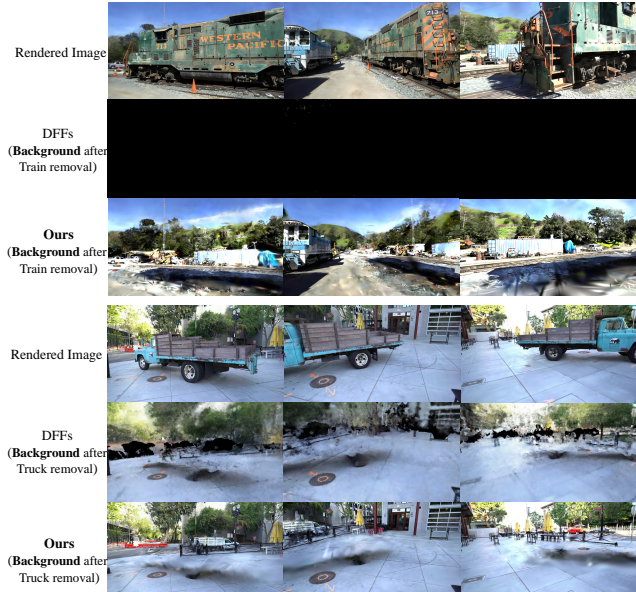


Figure 6. 3D Object removal on the Tanks&Temples dataset [16]. Comparing to DFFs [17], our Gaussian Grouping can remove the large-scale objects, such as tank, from the whole 3D scene with greatly reduced artifacts without leaving a blurry background.

Influence of the Identity Encoding In Table 2, we study the influence of our introduced Identity Encoding to original Gaussian Splatting’s 3D reconstruction performance and speed. The performance of Gaussian Grouping is on par with the original Gaussian Splatting method with negligible decrease, but it allows anything in the whole 3D scene to be segmented. By Identity Encoding, we lift the 2D zero-shot segmentation of SAM to 3D open world. Further, the grouped 3D Gaussians support a wide range of downstream editing tasks. We simply train all model components in an end-to-end manner jointly. This is different from Panoptic Lifting [20] which requires to block gradients from the segmentation branch back to the reconstruction branch.

Ablation on Identity Encoding Dimension We study the impact of dimension for our proposed Identity Encoding in Figure 4. To keep the training efficiency of Gaussian Grouping, we set the dimension of Identity Encoding to only 16 because it not only shows a good segmentation separation between objects but also keeps the training efficiency. Doubling dimension to 32 does not bring a better reconstruction quality compared to 16 but make training 1.3 times slower.

4.3. 3D Object Removal

3D object removal is to completely delete an object from the 3D scene, where the background behind the removed instance / stuff can be noisy or have a hole because of no observation. In Figure 6, we compare the removal effect of our Gaussian Grouping with the Distilled Feature Fields (DFFs) [17]. For challenging scene cases with large objects, our method can clearly separate the 3D object from the background scene. While the performance of DFFs is limited by the quality of its CLIP-distilled features, which results in the complete foreground removal (Train case) or inaccurate region removal with obvious artifacts (Truck case).

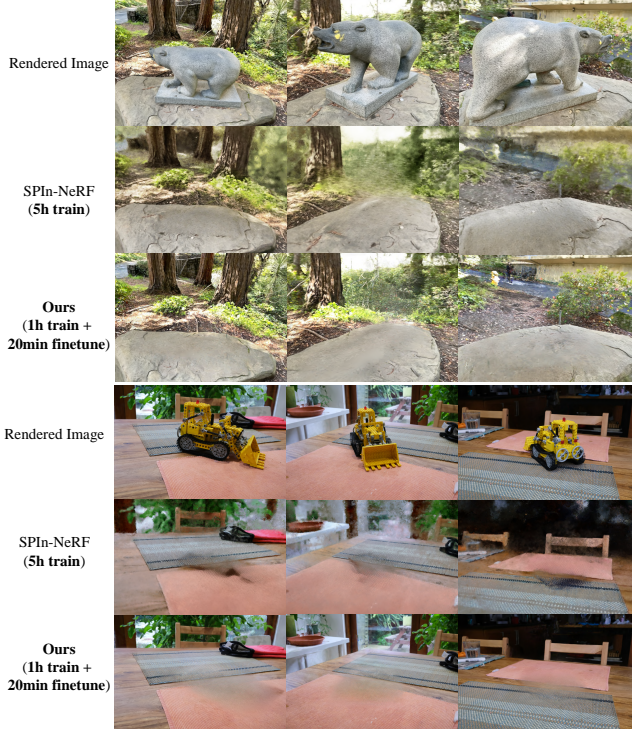


Figure 7. Comparison on 3D object inpainting cases, where SPIn-NeRF [31] requires 5h training while our method with better inpainting quality only needs 1 hour training and 20 minutes tuning.

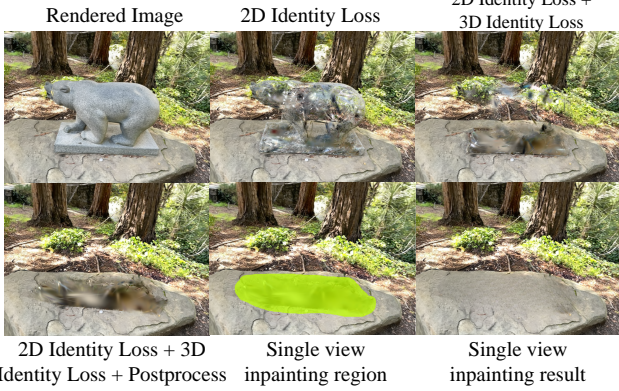


Figure 8. Ablation on the Grouping Loss on the Bear inpainting case. The joint supervision of 2D and 3D losses addresses the “transparent bear issue”, which shows better Gaussian Grouping accuracy. After deleting the Gaussians belong to the bear, we detect the image hole region with no Gaussians projection covering and then use LAMA [41] to produce single view inpainting result to guide the learning for newly added Gaussians.

4.4. 3D Object Inpainting

Based on the 3D object removal, in 3D object inpainting task, we aim to further fill the “hole regions” due to missing of observation and make it a photo-realistic and view-consistent natural 3D scene. We first detect the regions which are invisible in all views after deletion, and then inpaint these “invisible regions” instead of the whole “2D ob-



Figure 9. Multi-object editing within the same image, where we concurrently perform 3D object removal for objects in the red and yellow circle, and colorization for the glove in the purple circle.

ject regions”. In each rendering view, we adopt the 2D inpainted image to guide the learning of newly introduced 3D Gaussian. In Figure 7, compared to SPIn-NeRF [31], the inpainting result of our Gaussian Grouping better preserves spatial detail and multi-view coherence.

Visual Ablation on the Grouping Losses In Figure 8, we study the effect of our grouping loss components, where solely using 2D Identity Loss will result in the ‘transparent bear issue’. This is due to Gaussians inside bear will be occluded during rendering and cannot be supervised sufficiently. We address this issue by proposing 3D Identity Loss for joint training with the 2D loss.

4.5. 3D Multi-Object Editing

In Figure 9, we demonstrate multiple editing actions (like removing objects and colorization) on different Gaussian groups within the same 3D scene. These grouped 3D Gaussian representation enables simultaneous editing of several objects while maintaining non-interference among them.

Limitation Due to the lack of dynamic modeling and time-dependent updating, the proposed 3D Gaussian Grouping method is currently limited to the static 3D scene. Also, it would also be interested to further explore fully unsupervised 3D Gaussian grouping in the future.

5. Conclusion

We propose Gaussian Grouping, the first 3D Gaussian-based approach to jointly reconstruct and segment anything in the open-world 3D scene. We introduce an Identity Encoding for 3D Gaussians that is supervised both by 2D mask predictions from SAM and 3D spatial consistency. Based on this grouped and discrete 3D scene representation, we further show it can support versatile scene editing applications, such as 3D object removal, 3D object inpainting and scene recomposition, with both high-quality visual effect and good time efficiency.

6. Appendix

In this supplementary material, we first conduct additional experiment analysis of our Gaussian Grouping in Section 6.1, including 3D object style transfer and open-world segmentation comparison. Then, in Section 6.2, we describe the detailed process on annotating our proposed LERF-Mask datasets with the visualization of annotation examples. We further provide more detailed 3D object inpainting and style transfer pipeline description in Section 6.3. Finally, we illustrate the algorithm pseudocode of our Gaussian Grouping and more implementation details in Section 6.4, including the method limitation analysis. Please refer to our project page for extensive 3D results comparison.

6.1. Supplementary Experiments

3D Object Style Transfer Comparison Gaussian Grouping supports 3D object style transfer efficiently. We compare with the recent Instruct-NeRF2NeRF [10] on 3D object style transfer in Figure 10, using the same instruction prompt “turn the bear into a panda” and the same image guidance by InstructPix2Pix [2]. Gaussian Grouping produces more coherent and natural transferred “bear” across views. Since our Gaussian Grouping models “anything masks” of open-world 3D scene, including the bear, the spatial details of background regions (outside the bear) are also faithfully preserved by our method. While for Instruct-NeRF2NeRF, the large portion of background regions are unnecessarily getting blurry with degraded quality. We describe the detailed pipeline of 3D object style transfer in Section 6.3.

Segmentation Efficiency Comparison to SA3D We also compare the segmentation results with SA3D [4] on the proposed LERF-Mask dataset for open-world 3D segmentation. Our Gaussian Grouping shows great advantages in segmentation efficiency. Using the same machine, our Gaussian Grouping jointly segments all objects of the 3D scene in 9 minutes, while SA3D requires 35 minutes for each object due to its inverse rendering design in 3D voxel grids. To segmenting each object of the 3D scene, SA3D repeatedly needs a separate new training, which makes SA3D time-consuming and not user-friendly in multi-object segmentation or editing scenarios.

6.2. Details on the LERF-Mask Annotation

Annotation Pipeline To measure the segmentation or fine-grained localization accuracy in open-world 3D scene, we construct the LERF-Mask dataset based on the existing LERF-Localization [14] evaluation dataset, where we manually annotate three scenes from LERF-Localization with accurate masks instead of using coarse bounding boxes. For each 3D scene, we provide 7.7 text queries with corresponding GT mask label in average. We use Roboflow platform

for label annotation, and it uses SAM [15] as an auxiliary tool for interactive segmentation. Similar to the annotation used in LERF, for each of the 3 scenes, we choose 2-4 novel views for testing and annotating the rendering of novel views.

Annotation Examples All language prompts used for our LERF-Mask dataset evaluation are listed in Table 3, which contains 23 prompts in total. Also, we provide visualization on the mask annotations in Figure 11.

6.3. Steps of Object Inpainting & Style Transfer

3D Object Inpainting Pipeline For inpainting, we remove the 3D Gaussians of the selected target by using a Gaussian Grouping model well-trained for 3D reconstruction and segmentation and add new Gaussians for finetuning. The steps are as follows:

Step 1). Train the Gaussian Grouping model with our proposed 2D and 3D Identity Grouping loss.

Step 2). Select the target object for inpainting. For each Identity Encoding associated with a 3D Gaussian, we acquire its linear layer classification result. Subsequently, we remove those 3D Gaussians that are classified as the label of the selected object. Also, we remove the 3D Gaussians with position inside the convex hull of the object Gaussians.

Step 3). On the rendering views after the deletion of the object, we detect the “blurry hole” with Grounding-DINO [24] as the mask for 2D inpainting and use DEVA [7] for association. We use LAMA [41] inpainting on each view as the target for finetuning.

Step 4). After the 3D Gaussians of the target object are deleted, we clone 200K new Gaussians near the deletion region. We freeze the other Gaussians, and only finetune the newly introduced 3D Gaussians.

Step 5). During the finetuning, we employ L1 loss only in the outside regions of the object mask, and adopt LPIPS loss inside the bounding box of the object mask.

3D Object Style Transfer Pipeline For style transfer, we finetune the 3D Gaussians belong to the corresponding target by using a Gaussian Grouping model well-trained for 3D reconstruction and segmentation. The steps are as follows:

Step 1). Train our Gaussian Grouping model with our proposed 2D and 3D Identity Grouping loss.

Step 2). Select the target object for style transfer. For each Identity Encoding associated with a 3D Gaussian, we acquire its linear layer classification result. Subsequently, we only finetune those 3D Gaussians that are classified as the label of the selected object. Also, we finetune the 3D Gaussians with position inside the convex hull of the object Gaussians. The Gaussians irrelevant to the editing target are frozen. During finetuning, we freeze the 3D position of Gaussians and make other Gaussian parameters (color, variance, opacity, etc.) trainable.

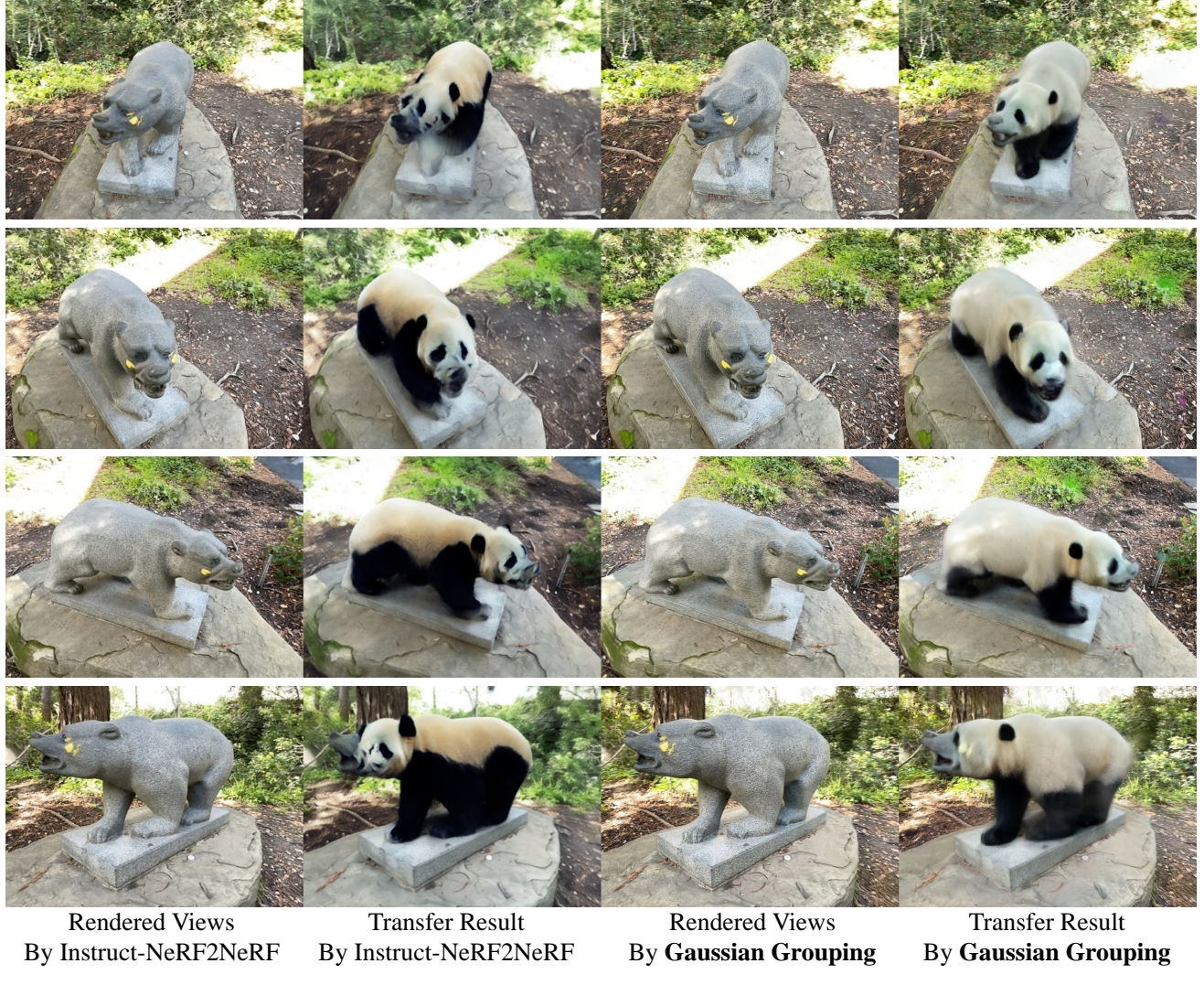


Figure 10. 3D object style transfer results comparison between Instruct-NeRF2NeRF [10] and our Gaussian Grouping under the same instruction prompt “Turn the bear into a panda” using InstructPix2Pix [2]. Our Gaussian Grouping produces more coherent and natural transfer results across views. Because Gaussian Grouping models the accurate mask of the bear, *the spatial details of background region (outside the bear) are more faithfully preserved* by our method.

Scene	Text queries		
Figurines	green apple porcelain hand rubber duck with red hat	green toy chair red apple	old camera red toy chair
Ramen	chopsticks pork belly	egg wavy noodles in bowl	glass of water yellow bowl
Teatime	apple cookies on a plate sheep tea in a glass	bag of cookies paper napkin spoon handle	coffee mug plate stuffed bear

Table 3. Prompt labels used during segmentation experiments in our proposed LERF-Mask dataset (23 total).



Figure 11. Annotation visualization of our proposed LERF-Mask dataset. We manually annotate three scenes from LERF-Localization [14] with accurate masks instead to replace the coarse bounding boxes in [10]. The text queries are detailed in Table 3.

Step 3). During the finetuning process, we dynamically update the target images using an image-level style transfer model that has been pre-trained. Specifically, we employ InstructPix2Pix[2], introducing a noise input composed of the rendered view combined with random noise. This approach involves conditioning the diffusion model on a ground truth image to enhance accuracy and consistency.

Step 4). To preserve the spatial details of the background

regions, rendering losses are exclusively performed within the mask of the style transfer target. On the 2D rendered view, we employ L1 loss inside the object mask and LPIPS loss within the bounding box that encloses the object mask.

6.4. More Implementation Details

More implementation details We implement Gaussian Grouping based on Gaussian Splatting [13]. We add a 16-

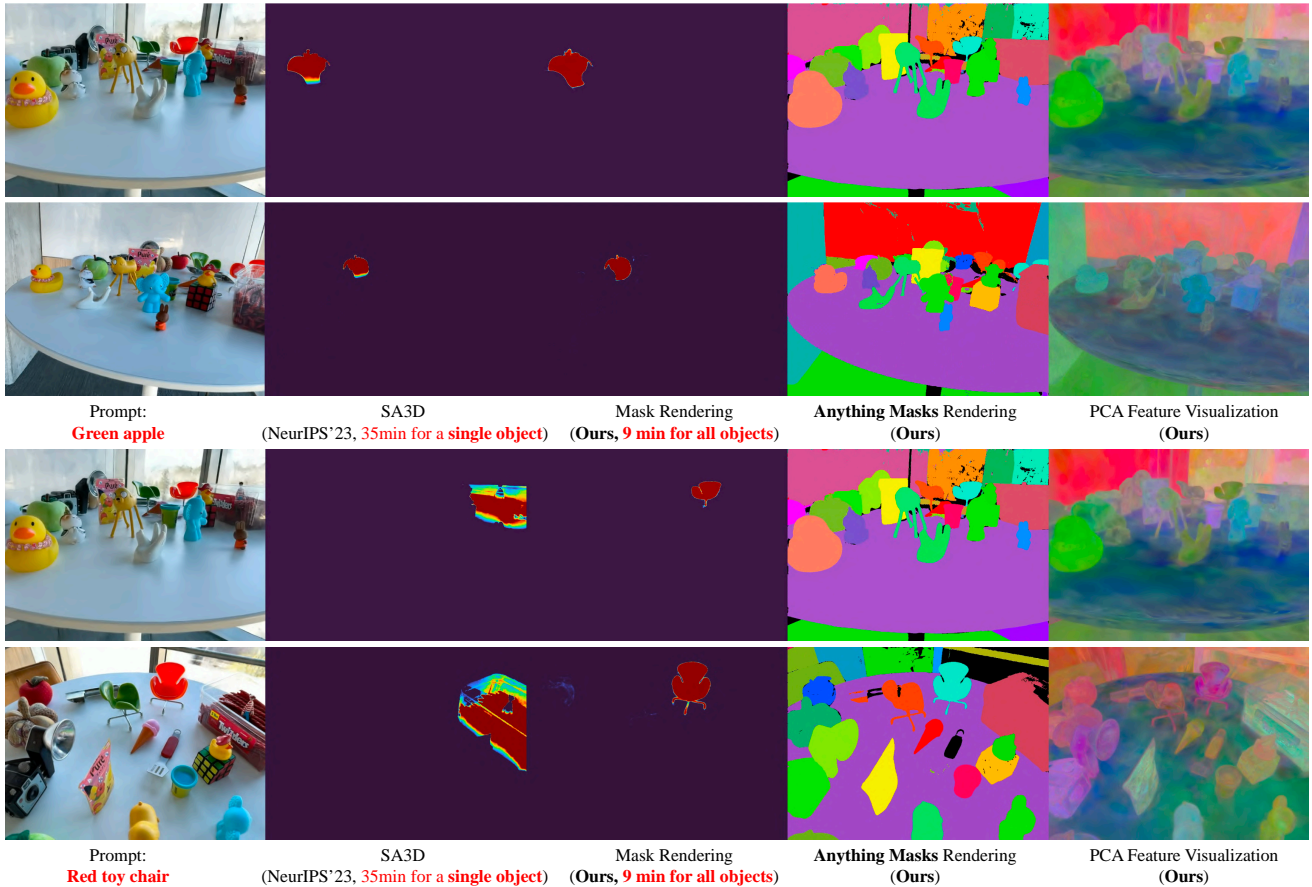


Figure 12. Segmentation comparison between SA3D [4] and our Gaussian Grouping on the rendering view. We adopt PCA to visualize the rendered Identity Encoding features in the rightmost column. *Note that SA3D does not support concurrent multi-object segmentation* due to its design limitation in the inverse rendering, which requires training and rendering for each segmentation target for around 35 minutes (~ 20 min for training and ~ 15 min for rendering). In contrast, our Gaussian Grouping shows great efficiency by segmenting all objects of the scene only in 9 minutes.

dimension identity encoding as a feature of each Gaussian, and implement forward and backward cuda rasterization similar to the direct current of Spherical Harmonics. The 3D Identity Encoding has a shape of $N * 1 * 16$, where N is the number of Gaussians. We set the degree of Spherical Harmonics to zero since instance identity does not change across views. The rendered 2D Identity Encoding has a shape of $16 * H * W$. 3D Identity Encoding and 2D Identity Encoding share the same identity classification linear layer with $(16, 256)$ input and output channels.

During training, we set $\lambda_{2d} = 1.0$ and $\lambda_{3d} = 2.0$. We use the Adam optimizer for both Gaussians and linear layer, with a learning rate of 0.0025 for identity encoding and 0.0005 for linear layer. For 3D regularization loss, we set nearest neighboring number to $k = 5$, and sampling points number to $m = 1000$. To improve efficiency and avoid calculating loss at boundary points, we downsample the point cloud to 300K to calculate the loss. All datasets are trained for 30K iterations on one A100 GPU.

Algorithm Pseudocode We outline the pseudocode for our

Gaussian Grouping in Algorithm 1, where we highlight the introduced core components in both red and bold texts. This idea of our Gaussian Grouping is simple to implement, and straightforward but producing an effective 3D representation to efficiently support versatile downstream scene editing tasks.

Limit Analysis Our Gaussian Grouping segments “anything masks” with the assistance of SAM. But the “anything mask labels” by original SAM [15] have no direct semantic language information. We adopt the Grounding-DINO[24] for open vocabulary segmentation to pick the 2D object, and match our anything masks rendering. When some language prompts are very complicated, the Grounding-DINO can not acquire the correct mask from the input text prompt and will give a wrong mask prediction. In this case, even if we provide the correct mask in anything mask rendering, we do not obtain explicit category information. Also, the zero-shot 2D association accuracy of DEVA [7] will also limit the open-world 3D segmentation performance of Gaussian Grouping. This can be solved by further improvement of

Algorithm 1 Gaussian Grouping

w, h : width and height of the training images

we employ a well-trained zero-shot tracker [7] to propagate and associate masks across views.

we follow the same Gaussians pruning and densification procedure in Gaussian Splatting [13].

```

 $p \leftarrow$  SfM Points                                 $\triangleright$  3D Positions
 $m = (m_1, m_2, \dots, m_K) \leftarrow$  SAM            $\triangleright$  SAM's Masks at Various  $K$  Views
 $(\hat{M}_1, \hat{M}_2, \dots, \hat{M}_K) \leftarrow$  Zero-shot Tracking(m)  $\triangleright$  Multi-view Associated Masks
 $s, \alpha, c, \mathbf{e} \leftarrow$  InitAttributes()           $\triangleright$  Covariances, Opacities, Colors, Identity Encodings
 $i \leftarrow 0$                                           $\triangleright$  Iteration Count
while not converged do
     $V, \hat{I}, \hat{M} \leftarrow$  SampleTrainingView()
     $I, \mathbf{E}_{\text{id}} \leftarrow$  Rasterize( $p, s, a, c, \mathbf{e}, V$ )
     $\mathcal{L}_{\text{image}} \leftarrow \mathcal{L}(I, \hat{I})$ 
     $\mathcal{L}_{\text{id}} \leftarrow \lambda_{2d}\mathcal{L}_{2d}(\mathbf{E}_{\text{id}}, \hat{M}) + \lambda_{3d}\mathcal{L}_{3d}(\mathbf{e})$   $\triangleright$  Camera View  $V$ , Image and Mask
     $\mathcal{L} \leftarrow \mathcal{L}_{\text{image}} + \mathcal{L}_{\text{id}}$   $\triangleright$  Rendered Image and Identity Encoding
     $p, s, a, c, \mathbf{e} \leftarrow$  Adam( $\nabla \mathcal{L}$ )            $\triangleright$  Original Image Rendering Loss
    if IsRefinementIteration( $i$ ) then
        for all  $J$  Gaussians  $(p_j, s_j, \alpha_j, c_j, \mathbf{e}_j)$  in  $(p, s, a, c, \mathbf{e})$  do
            if  $\alpha < \epsilon$  or IsTooLarge( $p_j, s_j$ ) then  $\triangleright$  Pruning
                RemoveGaussian()
            end if
            if  $\nabla_p \mathcal{L} > \tau_p$  then  $\triangleright$  Densification
                if  $\|S\| > \tau_S$  then  $\triangleright$  Over-reconstruction
                    SplitGaussian( $p_j, s_j, \alpha_j, c_j, e_j$ )
                else  $\triangleright$  Under-reconstruction
                    CloneGaussian( $p_j, s_j, \alpha_j, c_j, e_j$ )
                end if
            end if
        end for
    end if
     $i \leftarrow i + 1$ 
end while

```

the vision language detection model and better association schemes in the future.

References

[1] Jonathan T. Barron, Ben Mildenhall, Dor Verbin, Pratul P. Srinivasan, and Peter Hedman. Mip-nerf 360: Unbounded anti-aliased neural radiance fields. In *CVPR*, 2022. 6

[2] Tim Brooks, Aleksander Holynski, and Alexei A. Efros. Instructpix2pix: Learning to follow image editing instructions. In *CVPR*, 2023. 9, 10, 11

[3] Mathilde Caron, Hugo Touvron, Ishan Misra, Hervé Jégou, Julien Mairal, Piotr Bojanowski, and Armand Joulin. Emerging properties in self-supervised vision transformers. In *ICCV*, 2021. 2, 3

[4] Jiazhong Cen, Zanwei Zhou, Jiemin Fang, Chen Yang, Wei Shen, Lingxi Xie, Xiaopeng Zhang, and Qi Tian. Segment anything in 3d with nerfs. In *NeurIPS*, 2023. 2, 3, 9, 12

[5] Xiaokang Chen, Jiaxiang Tang, Diwen Wan, Jingbo Wang, and Gang Zeng. Interactive segment anything nerf with feature imitation. *arXiv preprint arXiv:2305.16233*, 2023. 3

[6] Zilong Chen, Feng Wang, and Huaping Liu. Text-to-3d using gaussian splatting. *arXiv preprint arXiv:2309.16585*, 2023. 2

[7] Ho Kei Cheng, Seoung Wug Oh, Brian Price, Alexander Schwing, and Joon-Young Lee. Tracking anything with decoupled video segmentation. In *ICCV*, 2023. 4, 6, 9, 12, 13

[8] Angela Dai, Angel X Chang, Manolis Savva, Maciej Halber, Thomas Funkhouser, and Matthias Nießner. Scannet: Richly-annotated 3d reconstructions of indoor scenes. In *CVPR*, 2017. 2

[9] Xiao Fu, Shangzhan Zhang, Tianrun Chen, Yichong Lu, Lanyun Zhu, Xiaowei Zhou, Andreas Geiger, and Yiyi Liao. Panoptic nerf: 3d-to-2d label transfer for panoptic urban scene segmentation. In *International Conference on 3D Vision (3DV)*, 2022. 3

[10] Ayaan Haque, Matthew Tancik, Alexei Efros, Aleksander Holynski, and Angjoo Kanazawa. Instruct-nerf2nerf: Editing 3d scenes with instructions. In *ICCV*, 2023. 3, 6, 9, 10, 11

[11] Kacper Kania, Kwang Moo Yi, Marek Kowalski, Tomasz Trzcinski, and Andrea Tagliasacchi. CoNeRF: Controllable Neural Radiance Fields. In *CVPR*, 2022. 3

[12] Lei Ke, Mingqiao Ye, Martin Danelljan, Yifan Liu, Yu-Wing Tai, Chi-Keung Tang, and Fisher Yu. Segment anything in high quality. In *NeurIPS*, 2023. 2

[13] Bernhard Kerbl, Georgios Kopanas, Thomas Leimkühler, and George Drettakis. 3d gaussian splatting for real-time radiance field rendering. *ACM TOG*, 42(4):1–14, 2023. 2, 3, 4, 5, 6, 11, 13

[14] Justin Kerr, Chung Min Kim, Ken Goldberg, Angjoo Kanazawa, and Matthew Tancik. Lerf: Language embedded radiance fields. In *ICCV*, 2023. 2, 3, 4, 6, 7, 9, 11

[15] Alexander Kirillov, Eric Mintun, Nikhila Ravi, Hanzi Mao, Chloe Rolland, Laura Gustafson, Tete Xiao, Spencer Whitehead, Alexander C Berg, Wan-Yen Lo, et al. Segment anything. In *ICCV*, 2023. 2, 3, 4, 9, 12

[16] Arno Knapitsch, Jaesik Park, Qian-Yi Zhou, and Vladlen Koltun. Tanks and temples: Benchmarking large-scale scene reconstruction. *ACM Transactions on Graphics (ToG)*, 36(4):1–13, 2017. 6, 7

[17] Sosuke Kobayashi, Eiichi Matsumoto, and Vincent Sitzmann. Decomposing nerf for editing via feature field distillation. In *NeurIPS*, 2022. 2, 3, 4, 6, 7

[18] Georgios Kopanas, Julien Philip, Thomas Leimkühler, and George Drettakis. Point-based neural rendering with per-view optimization. In *Computer Graphics Forum*, pages 29–43, 2021. 5

[19] Georgios Kopanas, Thomas Leimkühler, Gilles Rainer, Clément Jambon, and George Drettakis. Neural point cat-acaustics for novel-view synthesis of reflections. *ACM TOG*, 41(6):1–15, 2022. 5

[20] Abhijit Kundu, Kyle Genova, Xiaoqi Yin, Alireza Fathi, Caroline Pantofaru, Leonidas J Guibas, Andrea Tagliasacchi, Frank Dellaert, and Thomas Funkhouser. Panoptic neural fields: A semantic object-aware neural scene representation. In *Proceedings of the IEEE/CVF Conference on Computer Vision and Pattern Recognition*, pages 12871–12881, 2022. 3, 7

[21] Yuan Li, Zhi-Hao Lin, David Forsyth, Jia-Bin Huang, and Shenlong Wang. Climatenerf: Extreme weather synthesis in neural radiance field. In *ICCV*, 2023. 3

[22] Hao-Kang Liu, I Shen, Bing-Yu Chen, et al. Nerf-in: Free-form nerf inpainting with rgb-d priors. *arXiv preprint arXiv:2206.04901*, 2022. 3

[23] Steven Liu, Xiuming Zhang, Zhoutong Zhang, Richard Zhang, Jun-Yan Zhu, and Bryan Russell. Editing conditional radiance fields. In *ICCV*, 2021. 3

[24] Shilong Liu, Zhaoyang Zeng, Tianhe Ren, Feng Li, Hao Zhang, Jie Yang, Chunyu Li, Jianwei Yang, Hang Su, Jun Zhu, et al. Grounding dino: Marrying dino with grounded pre-training for open-set object detection. *arXiv preprint arXiv:2303.05499*, 2023. 6, 7, 9, 12

[25] Yichen Liu, Benran Hu, Junkai Huang, Yu-Wing Tai, and Chi-Keung Tang. Instance neural radiance field. In *ICCV*, 2023. 2

[26] Jonathon Luiten, Georgios Kopanas, Bastian Leibe, and Deva Ramanan. Dynamic 3d gaussians: Tracking by persistent dynamic view synthesis. *arXiv preprint arXiv:2308.09713*, 2023. 2

[27] Nelson Max. Optical models for direct volume rendering. *IEEE TVCG*, 1(2):99–108, 1995. 5

[28] Ben Mildenhall, Pratul P. Srinivasan, Rodrigo Ortiz-Cayon, Nima Khademi Kalantari, Ravi Ramamoorthi, Ren Ng, and Abhishek Kar. Local light field fusion: Practical view synthesis with prescriptive sampling guidelines. *ACM Transactions on Graphics (TOG)*, 2019. 6

[29] Ben Mildenhall, Pratul P. Srinivasan, Matthew Tancik, Jonathan T. Barron, Ravi Ramamoorthi, and Ren Ng. Nerf: Representing scenes as neural radiance fields for view synthesis. In *ECCV*, 2020. 2, 5

[30] Ashkan Mirzaei, Yash Kant, Jonathan Kelly, and Igor Gilitschenski. Laterf: Label and text driven object radiance fields. In *ECCV*, 2022. 3

[31] Ashkan Mirzaei, Tristan Aumentado-Armstrong, Konstantinos G Derpanis, Jonathan Kelly, Marcus A Brubaker, Igor

Gilitschenski, and Alex Levinshtein. Spin-nerf: Multiview segmentation and perceptual inpainting with neural radiance fields. In *CVPR*, 2023. 3, 6, 8

[32] Julian Ost, Fahim Mannan, Nils Thuerey, Julian Knodt, and Felix Heide. Neural scene graphs for dynamic scenes. In *CVPR*, 2021. 3

[33] Songyou Peng, Kyle Genova, Chiyu Jiang, Andrea Tagliasacchi, Marc Pollefeys, Thomas Funkhouser, et al. Openscene: 3d scene understanding with open vocabularies. In *CVPR*, 2023. 2

[34] Alec Radford, Jong Wook Kim, Chris Hallacy, Aditya Ramesh, Gabriel Goh, Sandhini Agarwal, Girish Sastry, Amanda Askell, Pamela Mishkin, Jack Clark, et al. Learning transferable visual models from natural language supervision. In *ICML*, 2021. 2, 3

[35] Daniel Rebain, Wei Jiang, Soroosh Yazdani, Ke Li, Kwang Moo Yi, and Andrea Tagliasacchi. Derf: Decomposed radiance fields. In *CVPR*, 2021. 3

[36] Robin Rombach, Andreas Blattmann, Dominik Lorenz, Patrick Esser, and Björn Ommer. High-resolution image synthesis with latent diffusion models. In *CVPR*, 2022. 2

[37] Jonas Schult, Francis Engelmann, Alexander Hermans, Or Litany, Siyu Tang, and Bastian Leibe. Mask3D: Mask Transformer for 3D Semantic Instance Segmentation. In *ICRA*, 2023. 2

[38] QiuHong Shen, Xingyi Yang, and XinChao Wang. Anything-3d: Towards single-view anything reconstruction in the wild. *arXiv preprint arXiv:2304.10261*, 2023. 2

[39] Yawar Siddiqui, Lorenzo Porzi, Samuel Rota Bulò, Norman Müller, Matthias Nießner, Angela Dai, and Peter Kontschieder. Panoptic lifting for 3d scene understanding with neural fields. In *CVPR*, 2023. 2, 3, 4, 6

[40] Noah Snavely, Steven M Seitz, and Richard Szeliski. Photo tourism: exploring photo collections in 3d. In *ACM siggraph*, 2006. 4

[41] Roman Suvorov, Elizaveta Logacheva, Anton Mashikhin, Anastasia Remizova, Arsenii Ashukha, Aleksei Silvestrov, Naejin Kong, Harshith Goka, Kiwoong Park, and Victor Lempitsky. Resolution-robust large mask inpainting with fourier convolutions. In *WACV*, 2022. 5, 8, 9

[42] Ayça Takmaz, Elisabetta Fedele, Robert W. Sumner, Marc Pollefeys, Federico Tombari, and Francis Engelmann. Open-Mask3D: Open-Vocabulary 3D Instance Segmentation. In *NeurIPS*, 2023. 2

[43] Jiaxiang Tang, Jiawei Ren, Hang Zhou, Ziwei Liu, and Gang Zeng. Dreamgaussian: Generative gaussian splatting for efficient 3d content creation. *arXiv preprint arXiv:2309.16653*, 2023. 2

[44] Vadim Tschernezki, Iro Laina, Diane Larlus, and Andrea Vedaldi. Neural feature fusion fields: 3d distillation of self-supervised 2d image representations. *arXiv preprint arXiv:2209.03494*, 2022. 3

[45] Vadim Tschernezki, Iro Laina, Diane Larlus, and Andrea Vedaldi. Neural feature fusion fields: 3D distillation of self-supervised 2D image representations. In *International Conference on 3D Vision (3DV)*, 2022.

[46] Suhani Vora, Noha Radwan, Klaus Greff, Henning Meyer, Kyle Genova, Mehdi S. M. Sajjadi, Etienne Pot, Andrea Tagliasacchi, and Daniel Duckworth. Nesf: Neural semantic fields for generalizable semantic segmentation of 3d scenes, 2021. 3

[47] Bing Wang, Lu Chen, and Bo Yang. Dm-nerf: 3d scene geometry decomposition and manipulation from 2d images. *arXiv preprint arXiv:2208.07227*, 2022. 3

[48] Can Wang, Menglei Chai, Mingming He, Dongdong Chen, and Jing Liao. Clip-nerf: Text-and-image driven manipulation of neural radiance fields. In *CVPR*, 2022. 3

[49] Guanjun Wu, Taoran Yi, Jiemin Fang, Lingxi Xie, Xiaopeng Zhang, Wei Wei, Wenyu Liu, Qi Tian, and Xinggang Wang. 4d gaussian splatting for real-time dynamic scene rendering. *arXiv preprint arXiv:2310.08528*, 2023. 2

[50] Bangbang Yang, Yinda Zhang, Yinghao Xu, Yijin Li, Han Zhou, Hujun Bao, Guofeng Zhang, and Zhaopeng Cui. Learning object-compositional neural radiance field for editable scene rendering. In *ICCV*, 2021. 3

[51] Yunhan Yang, Xiaoyang Wu, Tong He, Hengshuang Zhao, and Xihui Liu. Sam3d: Segment anything in 3d scenes. *arXiv preprint arXiv:2306.03908*, 2023. 3

[52] Ziyi Yang, Xinyu Gao, Wen Zhou, Shaohui Jiao, Yuqing Zhang, and Xiaogang Jin. Deformable 3d gaussians for high-fidelity monocular dynamic scene reconstruction. *arXiv preprint arXiv:2309.13101*, 2023. 2

[53] Zeyu Yang, Hongye Yang, Zijie Pan, Xiatian Zhu, and Li Zhang. Real-time photorealistic dynamic scene representation and rendering with 4d gaussian splatting. *arXiv preprint arXiv:2310.10642*, 2023. 2

[54] Taoran Yi, Jiemin Fang, Guanjun Wu, Lingxi Xie, Xiaopeng Zhang, Wenyu Liu, Qi Tian, and Xinggang Wang. Gaussian-dreamer: Fast generation from text to 3d gaussian splatting with point cloud priors. *arXiv preprint arXiv:2310.08529*, 2023. 2

[55] Wang Yifan, Felice Serena, Shihao Wu, Cengiz Öztïrelı, and Olga Sorkine-Hornung. Differentiable surface splatting for point-based geometry processing. *ACM Transactions on Graphics (TOG)*, 38(6):1–14, 2019. 5

[56] Hong-Xing Yu, Leonidas J Guibas, and Jiajun Wu. Unsupervised discovery of object radiance fields. *arXiv preprint arXiv:2107.07905*, 2021. 3

[57] Yu-Jie Yuan, Yang-Tian Sun, Yu-Kun Lai, Yuewen Ma, Rongfei Jia, and Lin Gao. Nerf-editing: geometry editing of neural radiance fields. In *CVPR*, 2022. 3

[58] Chaoning Zhang, Dongshen Han, Yu Qiao, Jung Uk Kim, Sung-Ho Bae, Seungkyu Lee, and Choong Seon Hong. Faster segment anything: Towards lightweight sam for mobile applications. *arXiv preprint arXiv:2306.14289*, 2023. 2

[59] Jiakai Zhang, Xinhang Liu, Xinyi Ye, Fuqiang Zhao, Yan-shun Zhang, Minye Wu, Yingliang Zhang, Lan Xu, and Jingyi Yu. Editable free-viewpoint video using a layered neural representation. *ACM Transactions on Graphics (TOG)*, 40(4):1–18, 2021. 3

[60] Shuaifeng Zhi, Tristan Laidlow, Stefan Leutenegger, and Andrew J. Davison. In-place scene labelling and understanding with implicit scene representation. In *ICCV*, 2021. 2

[61] Matthias Zwicker, Hanspeter Pfister, Jeroen Van Baar, and Markus Gross. Surface splatting. In *Proceedings of the 28th annual conference on Computer graphics and interactive techniques*, pages 371–378, 2001. 5